

Common and uncommon vascular rings and slings: a multi-modality review

Jonathan R. Dillman · Anil K. Attili · Prachi P. Agarwal ·
Adam L. Dorfman · Ramiro J. Hernandez ·
Peter J. Strouse

Received: 23 February 2011 / Revised: 7 April 2011 / Accepted: 11 April 2011 / Published online: 19 May 2011
© Springer-Verlag 2011

Abstract Vascular rings and pulmonary slings are congenital anomalies of the aortic arch/great vessels and pulmonary arteries, respectively, that commonly present early during infancy and childhood with respiratory and/or feeding difficulties. The diagnosis of these conditions frequently utilizes a multi-modality radiological approach, commonly utilizing some combination of radiography, esophagography, CT angiography and MR angiography. The purpose of this pictorial review is to illustrate the radiological findings of *common* and *uncommon* vascular rings and pulmonary slings in children using a state-of-the-art multi-modality imaging approach.

CME activity

This article has been selected as the CME activity for the current month. Please visit the SPR Web site at www.pedrad.org on the Education page and follow the instructions to complete this CME activity.

J. R. Dillman (✉) · P. P. Agarwal · A. L. Dorfman ·
R. J. Hernandez · P. J. Strouse
Department of Radiology, Section of Pediatric Radiology,
University of Michigan Health System,
C.S. Mott Children's Hospital,
1500 E. Medical Center Drive,
Ann Arbor, MI 48109–5252, USA
e-mail: jonadill@med.umich.edu

A. L. Dorfman
Department of Pediatrics and Communicable Diseases, Division
of Pediatric Cardiology, University of Michigan Health System,
C.S. Mott Children's Hospital,
Ann Arbor, MI, USA

A. K. Attili
Department of Radiology,
University of Kentucky College of Medicine,
Lexington, KY, USA

Keywords Vascular ring · Pulmonary sling · Children · MR angiography · CT angiography · Esophagography · Radiography

Introduction

Vascular rings and pulmonary slings are relatively rare congenital anomalies of the aortic arch and great vessels and the pulmonary arteries, respectively. Both conditions commonly present during infancy or early childhood with respiratory difficulties (e.g., stridor or wheezing), recurrent pulmonary infections and difficulty feeding [1, 2]. A *vascular ring* is defined as an abnormal encircling of the trachea and esophagus by the aortic arch and its branches (or remnants) [1–4], while a *pulmonary sling* is present when the left pulmonary artery arises anomalously from the right pulmonary artery [1, 5–8]. The radiological work-up and diagnosis of these vascular anomalies most commonly relies upon a multi-modality approach, often using some combination of radiography, esophagography (barium swallow), computed tomography angiography (CTA) and magnetic resonance angiography (MRA). Three-dimensional (3-D) renderings of CTA and MRA data sets have made catheter-based angiography nearly obsolete for the diagnosis of these conditions and necessary surgical planning [4, 9], and these imaging techniques have sensitivities approaching 100% [9]. The purpose of this review is to illustrate the radiological findings of *common* and *uncommon* vascular rings and pulmonary slings in children using a state-of-the-art multi-modality imaging approach.

CTA vs. MRA

Both CTA and MRA excellently depict vascular rings and pulmonary slings. While CTA allows for rapid imaging that can minimize motion-related artifacts and lessen the need for sedation, it does utilize ionizing radiation for image creation [2]. Low kilovolt potential (kVp) imaging, automatic tube current modulation (a form of automatic exposure control) to minimize mA and certain image reconstruction techniques (such as adaptive statistical iterative reconstruction, or ASIR) can be used to mitigate radiation-related risks, however. MRA does not utilize ionizing radiation to produce images, but frequently requires deep conscious sedation or general anesthesia in younger and uncooperative children and is generally considered to be a more technically demanding study [2]. MRA is also associated with longer examination times, higher costs, limited availability and slightly poorer spatial resolution [2, 10]. Both CTA and MRA allow for visualization of the central airways [9, 11] and the creation of isotropic multi-planar reformatted and 3-D reconstructed images that can assist with defining vascular anatomy and surgical planning. Our institutional vascular ring CTA and MRA protocols are provided in Tables 1 and 2. When these imaging studies are performed under general anesthesia, stenting of the narrowed portion of the airway with an endotracheal tube should be avoided if possible.

Table 1 Institutional vascular ring CTA protocol^a

Scanner mode	helical
Gantry rotation time	0.5 sec
Detector configuration	64×0.625 mm
Pitch	1.375:1
Speed	27.5 mm/rotation
kVp	80–100
mA	ATCM ^b
Noise index	28–33.6
ASIR ^c	single slice, 30%
Contrast volume	2 ml/kg
Injection rate ^d	1–3 ml/sec
Contrast timing ^d	bolus tracking on aortic arch ^e
Image reconstruction	2.5 mm thickness every 1.25 mm

^a Using GE Healthcare (Waukesha, WI) Discovery CT750 HD 64-channel scanner

^b ATCM = automatic tube current modulation

^c ASIR = adaptive statistical iterative reconstruction

^d when using a power injector; hand injection of IV contrast material is performed in neonates and very small children

^e 100 Hounsfield unit (HU) enhancement threshold; bolus tracking is performed on main pulmonary artery in suspected pulmonary sling

Table 2 Institutional vascular ring MRA protocol^a

1. 3-plane localizer
2. Proton density (PD)-weighted fast spin-echo (FSE)—black blood imaging
 - axial and coronal planes
 - free breathing
 - slice thickness (mm)=2.5–4.0
 - TR/TE (msec)=2 × R-R interval / 40
 - NSA=2
 - parallel imaging acceleration factor = none
3. 3-D balanced steady-state free precession (3-D SSFP)—bright blood imaging
 - sagittal plane
 - navigator-gated
 - slice thickness (mm)=1.2–1.6 (isotropic voxels)
 - TR/TE (msec)=4 / 2
 - NSA=1
 - parallel imaging acceleration factor=2
4. Dynamic 3-D MRA
 - sagittal (or coronal) plane
 - breath-held
 - slice thickness (mm)=2 (reconstructed every 1 mm)
 - TR/TE (msec)=5.7 / 1.8
 - NSA=1
 - parallel imaging acceleration factor=2

TR repetition time; TE echo time; NSA number of signal averages

^a Using Philips (Andover, MA) 1.5 Tesla Achieva MRI scanner with parallel imaging (SENSE)

Coil selection is based on patient weight:

<3 kg—8-channel knee coil

3–10 kg—2-channel Flex M coil

>10 kg—either 5-channel cardiac coil or 16-channel torso coil

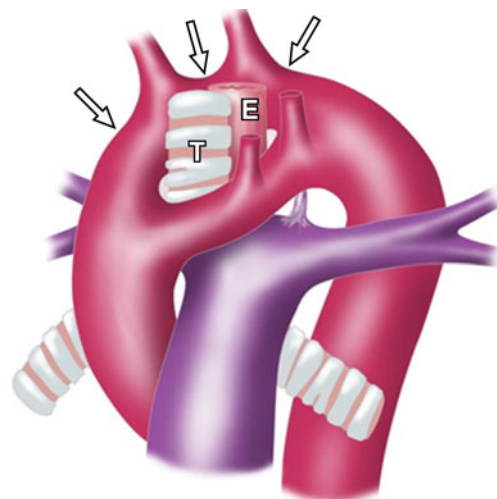
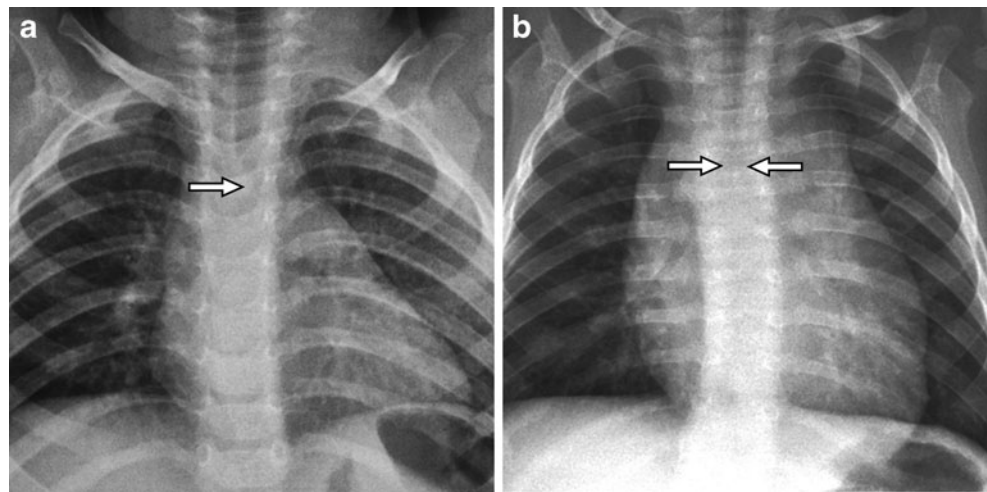


Fig. 1 Illustration of classic double aortic arch. The trachea (T) and esophagus (E) are surrounded by bilateral aortic arches, and the right aortic arch (white arrows) is both higher in location and larger in caliber. The right common carotid and right subclavian arteries arise from the right aortic arch, while the left common carotid and left subclavian arteries arise from the left aortic arch

Fig. 2 Frontal radiographs demonstrate double aortic arch. **a** An 18-month-old girl with extrinsic impression on the right lateral aspect of the trachea (arrow), proved to represent a double aortic arch. **b** A 5-month-old boy with narrowed midline trachea (arrows) due to a double aortic arch



Vascular rings

A vascular ring is present when there is abnormal encirclement of the trachea and esophagus by the aortic arch and its branches (or remnants) [1, 3, 4]. While loose vascular rings may remain asymptomatic and go undetected, tight vascular rings may cause significant symptoms due to extrinsic mass effect upon the airway and esophagus [2]. Vascular rings most commonly present with respiratory symptoms and dysphagia [1–4]. A *double aortic arch* is the most commonly detected symptomatic vascular ring, followed by a *right aortic arch with an aberrant left subclavian artery* (with intact ligamentum arteriosum) [1, 9]. Other vascular rings are much less common. The presence of a vascular ring should be suspected in the presence of an aortic diverticulum or when the aorta descends on the opposite side of the aortic arch [9].

Double aortic arch

The double aortic arch is the most common symptomatic vascular ring [1–3, 9]. The presence of bilateral aortic arches is likely due to persistence of both the right and left embryonic fourth aortic (branchial) arches [4, 11]. This vascular anomaly is most commonly isolated and is uncommonly associated with congenital heart disease [2, 3, 11]. Double aortic arches are usually symptomatic and are frequently detected in infancy.

In the classical variant (approximately 70%), the right aortic arch is dominant, being more cephalad in location and larger in caliber (Fig. 1) [3, 4, 9, 11]. The left aortic arch is usually smaller in caliber and may be atretic (persisting as a band of fibrous tissue) [4, 11–13]. An atretic segment may be located between the left common and left subclavian arteries mimicking a right aortic arch

with an aberrant left subclavian artery or distal to the left subclavian artery mimicking a right aortic arch with mirror-image branching and intact retroesophageal left ligamentum arteriosum. A study by Holmes et al. [14] demonstrated that there may be distortion and abnormal angulation of the proximal left subclavian artery due to traction from an atretic left arch. Occasionally, double aortic arches may be left aortic arch dominant or codominant. The establishment of aortic arch dominance is important as surgical thoracotomy and transection of the vascular ring are usually performed on the nondominant side [2]. The descending thoracic aorta is most commonly located on the left [2, 11].

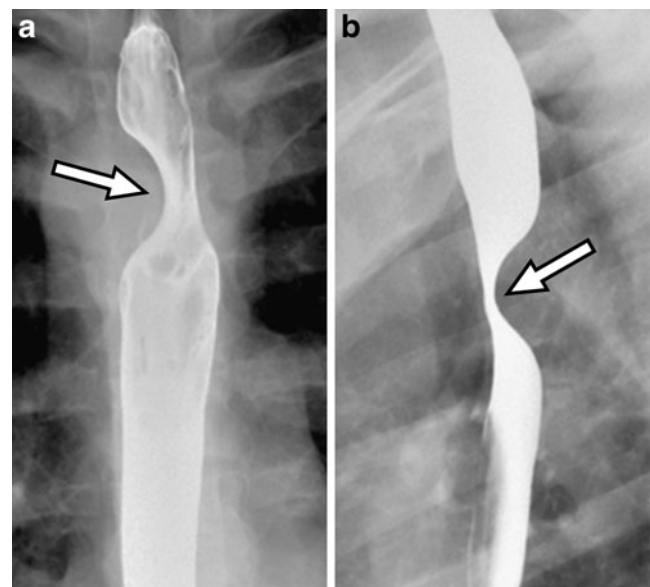


Fig. 3 Images in a 17-year-old girl with (a) right lateral and (b) posterior esophageal indentations at esophagography (arrows), proved to represent a double aortic arch

On frontal radiographs, the presence of a right or bilateral aortic knobs can suggest the presence of a double aortic arch (Fig. 2) [2, 9]. Bilateral aortic arches can also cause the trachea to be located abnormally in the midline (Fig. 2) [11]. Abnormal mass effect upon the airway by the vascular ring may cause supracarinal tracheal narrowing [2] as well as occasional congenital pulmonary overinflation due to air-trapping. On lateral radiographs, the lower trachea may appear narrowed with anterior bowing [1, 2, 11].

At esophagography, right lateral or bilateral esophageal indentations are observed at the expected level of the aortic arch (Fig. 3) [1, 2, 4, 11]. Esophagography in the lateral

projection demonstrates an abnormal posterior esophageal indentation (Fig. 3) [1, 2, 4, 9, 11].

A variety of CTA and MRA findings can be observed in the setting of a double aortic arch (Figs. 4 and 5). First, the bilateral aortic arches can be directly visualized and are well depicted by 3-D volume-rendered and maximum-intensity projection (MIP) reconstructed images. CTA and MRA both allow for the precise determination of aortic arch dominance (Fig. 6), a finding that has important surgical implications. Additionally, both CTA and MRA can suggest the presence of an atretic aortic arch segment. An aortic diverticulum helps to confirm the presence of a vascular ring (Figs. 7 and 8). Second, on axial imaging, all

Fig. 4 Double aortic arch in a 2-month-old girl. **a** An axial CTA image demonstrates symmetrical arrangement of the aortic branch vessels, the 4-artery sign. **b, c** Additional axial CTA images demonstrate bilateral aortic arches (*white arrows*) surrounding the airway and esophagus. There is moderate anteroposterior airway narrowing at the level of the carina (*black arrow*). **d** A 3-D volume-rendered CTA image (posterior view) confirms the presence of a double aortic arch

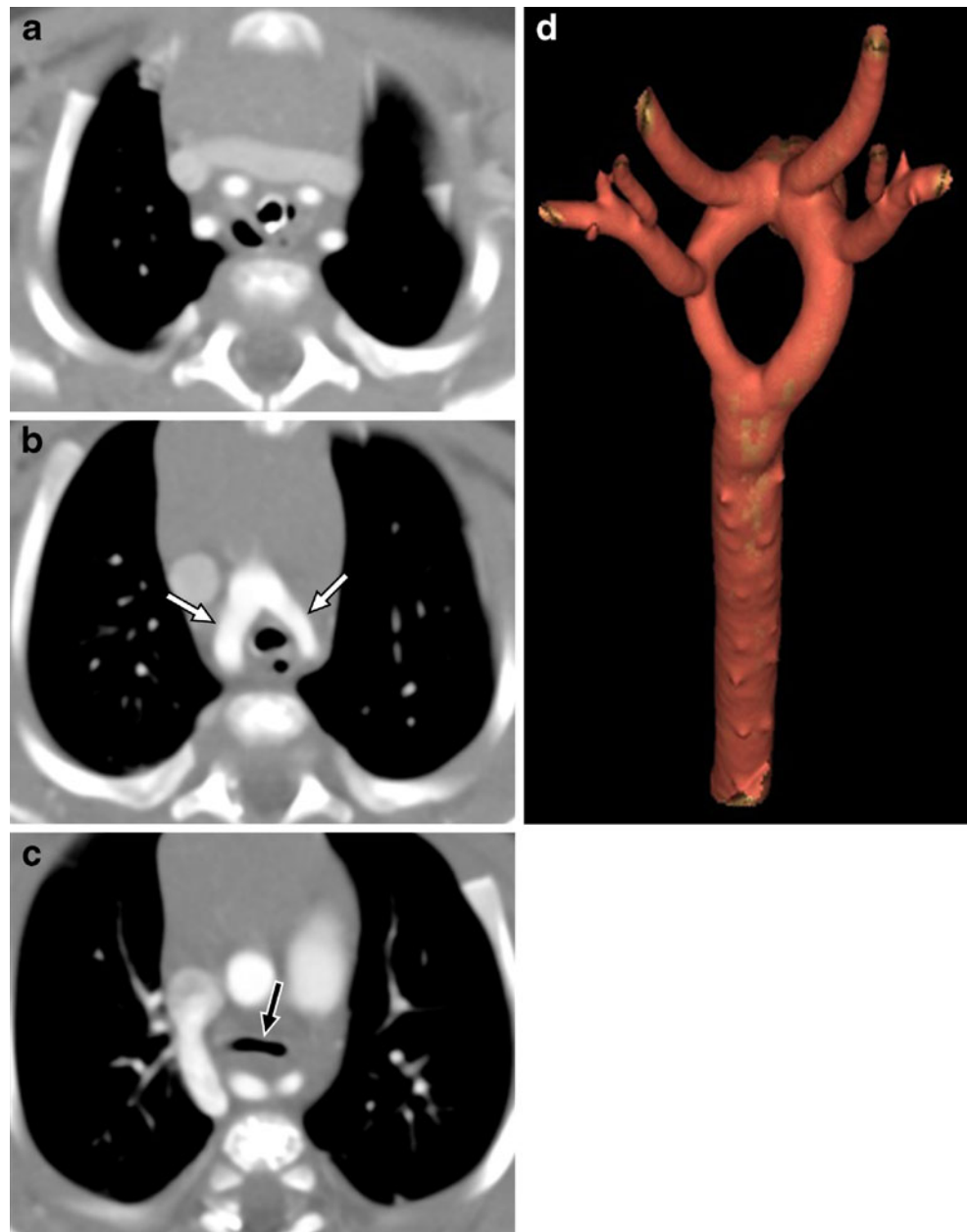


Fig. 5 Right-dominant double aortic arch in a 6-month-old boy. **a** An axial black blood image demonstrates the symmetrical arrangement of the aortic branch vessels, the four-artery sign. **b, c** Additional axial and coronal black blood images demonstrate bilateral aortic arches (*white arrows*) surrounding the airway and esophagus. There is at least moderate airway narrowing just above the level of the carina (*black arrow*). **d** A 3-D volume-rendered MRA image (superoposterior view) confirms the presence of a vascular ring

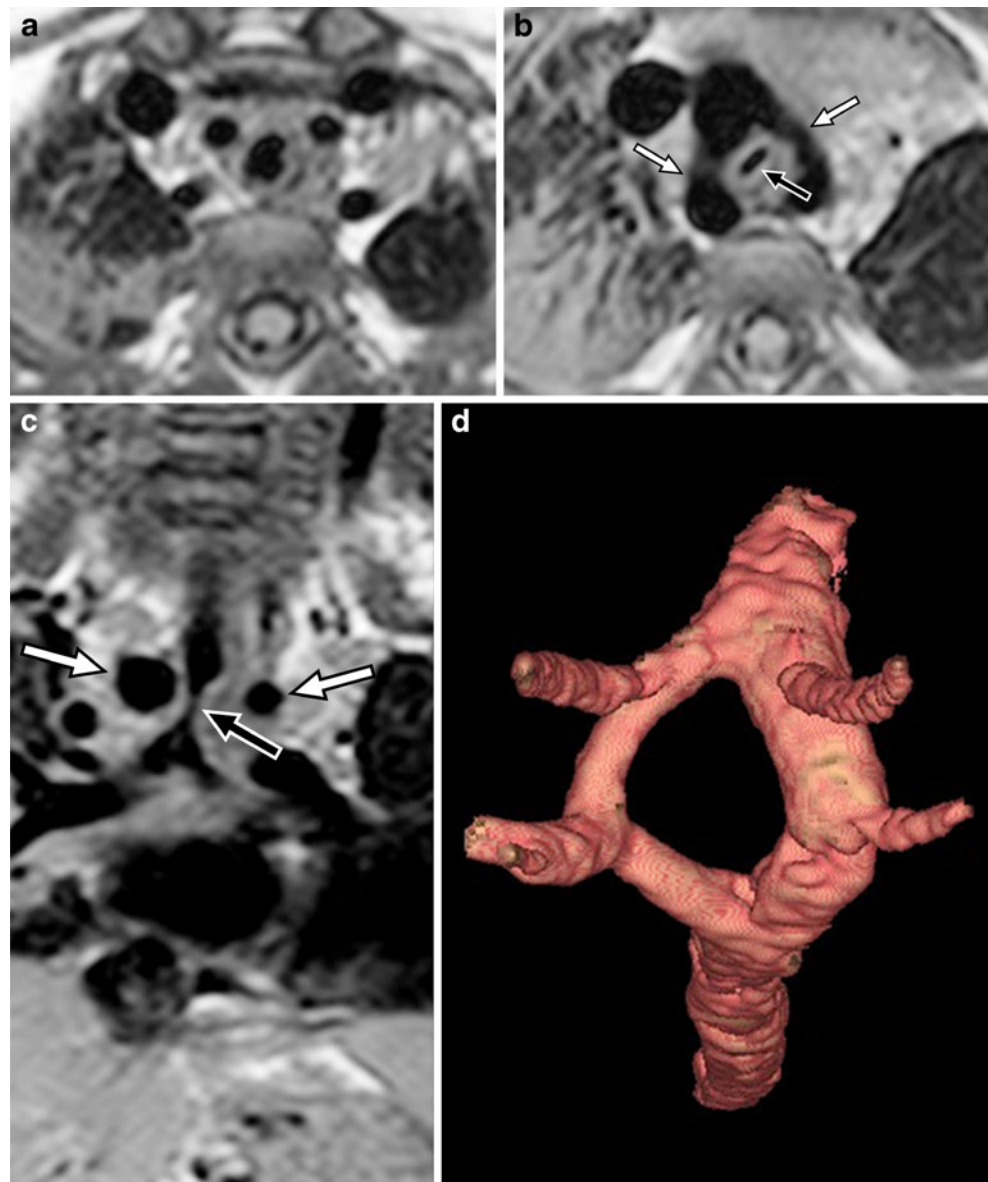


Fig. 6 Left-dominant double aortic arch in an 8-day-old boy. An axial subvolume maximum-intensity projection (MIP) CTA image demonstrates a diminutive right aortic arch, and there is marked tracheal narrowing (*arrow*). Please note, the degree of airway narrowing may be slightly overestimated on MIP images

four major brachio-cephalic aortic arch branches (the bilateral common carotid and subclavian arteries) are seen separately just above the expected level of the aortic arch having a symmetrical, trapezoid (or square) appearance, the four-artery sign [2, 9]. Finally, variable degrees of airway narrowing may be observed (most commonly affecting the lower trachea and carina). This finding is best appreciated on axial and coronal reformatted CTA as well as black blood and 3-D steady-state free precession (3-D SSFP) MRA images.

Right aortic arch with aberrant left subclavian artery

While a right aortic arch with an aberrant left subclavian artery is the second most common symptomatic vascular ring [9], it is commonly asymptomatic due to the vascular



Fig. 7 Double aortic arch in a 17-month-old girl. **a** A 3-D volume-rendered CTA image (posterior view) suggests an atretic left aortic arch segment (*curved line*) and aortic diverticulum (*arrow*). There is abnormal angulation/distortion of the proximal left subclavian artery. **b** A 3-D volume-rendered image of the airway confirms narrowing at the level of the carina due to extrinsic compression (*arrow*)

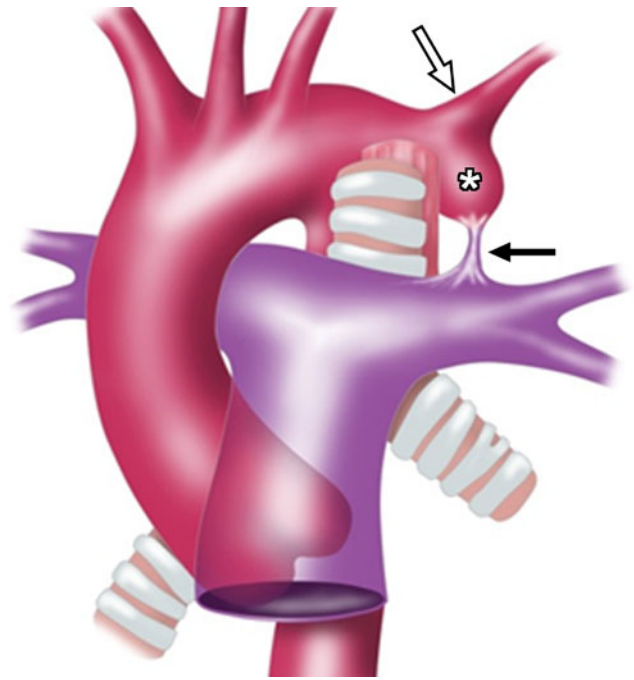


Fig. 9 Illustration of right aortic arch with aberrant left subclavian artery. The left subclavian artery (*white arrow*) is the last major vessel to originate from the aortic arch, arising from an aortic diverticulum (*). An intact ligamentum arteriosum completes the vascular ring (*black arrow*)

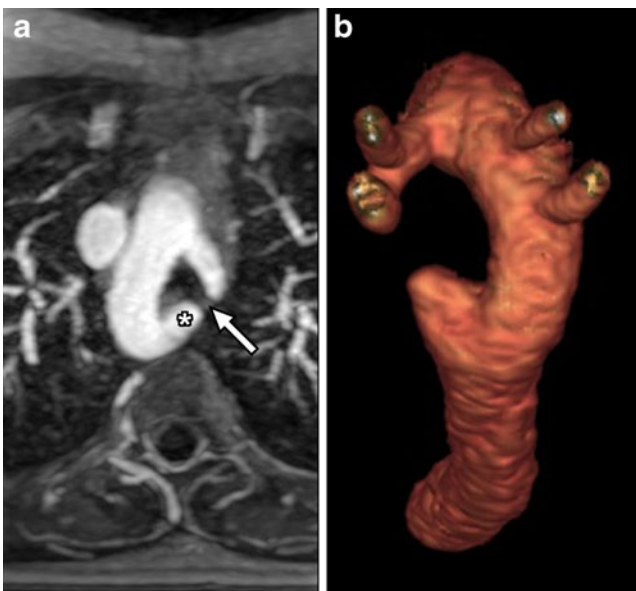


Fig. 8 Double aortic arch in a 13-year-old boy. **a** An axial subvolume MIP MRA image reveals an atretic left aortic arch segment (*white arrow*) and aortic diverticulum (*). **b** A 3-D volume-rendered MRA image (superoposterior view) confirms the MIP image findings

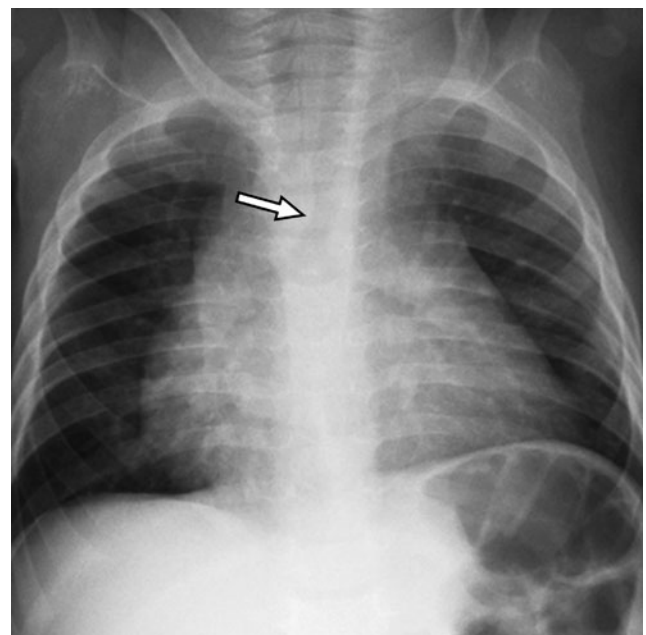


Fig. 10 Chest radiograph in a 5-month-old boy. The aortic arch has mass effect upon the right lateral aspect of the trachea (*arrow*)

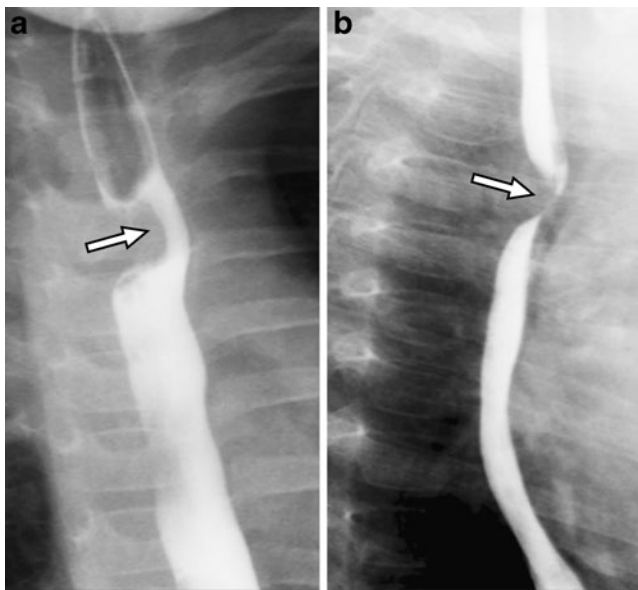


Fig. 11 Images in a 2-year-old girl with abnormal (a) right lateral and (b) posterior esophageal indentations (arrows) proved to be caused by a right aortic arch with an aberrant left subclavian artery

ring being relatively loose [11]. This vascular anomaly is usually isolated, and it is proposed to be due to interruption of “Edwards’ hypothetical left arch” between the left common carotid and left subclavian arteries [2, 3]. With this aortic arch configuration, the left subclavian artery is the last major branch to arise from the aortic arch, originating from bulbous aortic diverticulum and passing posterior to the esophagus (Fig. 9) [1, 2, 11]. The vascular ring is made complete by an intact left-side ligamentum arteriosum [1, 2].

On frontal radiographs, a right-side aortic knob is present (Fig. 10) [1, 2]. At lateral radiography, a mass-like opacity posterior to the trachea and above aortic arch (within the retrotracheal space or Raider triangle) may be observed.

At esophagography, abnormal right lateral and posterior esophageal indentations are present (Fig. 11) [1, 2, 4]. The abnormal posterior indentation may be oblique and angled toward the left shoulder [4]. The normal left lateral esophageal indentation is conspicuously absent.

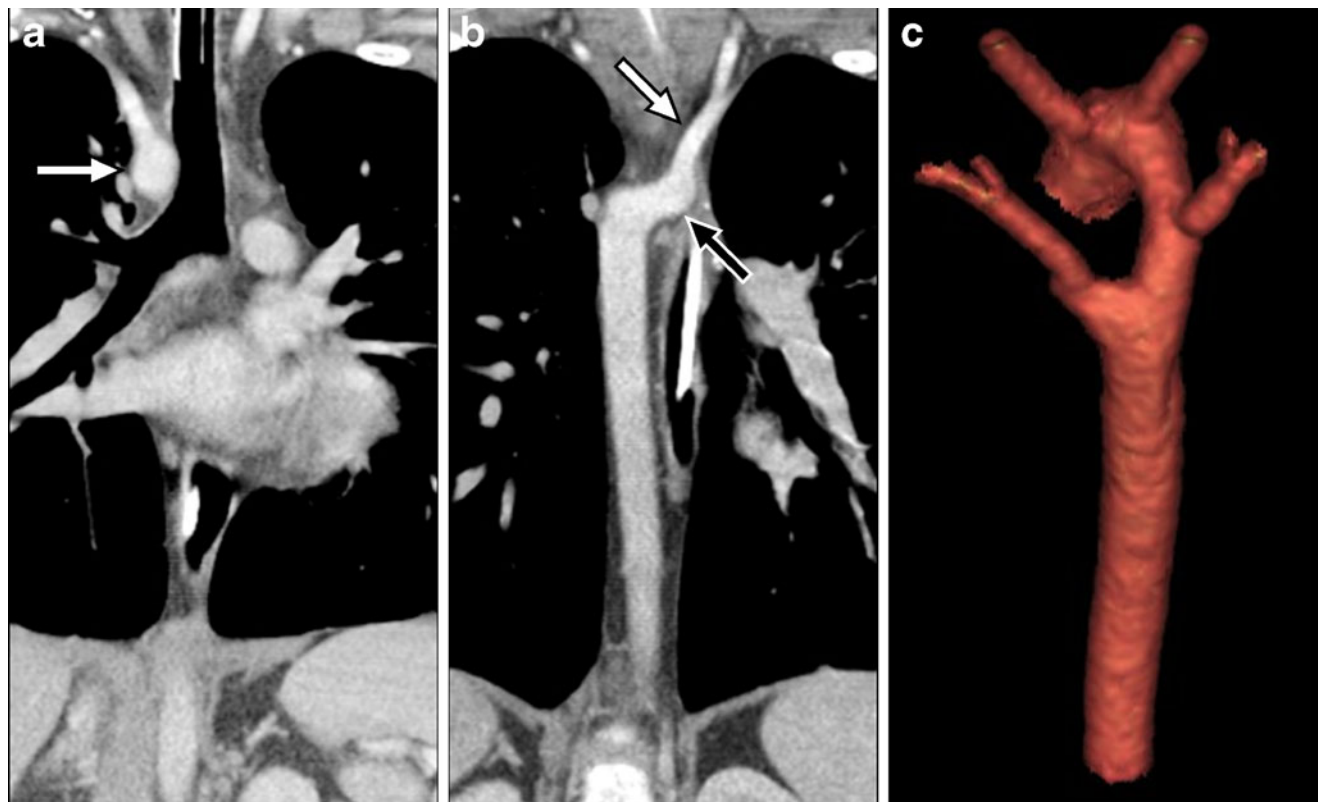


Fig. 12 Right aortic arch and aberrant left subclavian artery in a 2-year-old girl. **a** A coronal reformatted CTA image confirms that the aortic arch is on the right (arrow). There is only minimal narrowing of the trachea. **b** Another coronal reformatted image shows an aberrant

retroesophageal left subclavian artery (white arrow) arising from an aortic diverticulum (black arrow). **c** A 3-D volume-rendered CTA image (posterior view) confirms these findings

This vascular ring demonstrates similar findings at CTA and MRA (Figs. 12 and 13). First, the right aortic arch can be directly visualized, giving rise to four separate brachiocephalic branch vessels. Second, the left subclavian artery is the last major aortic arch branch vessel, originating from

an aortic diverticulum and having a retroesophageal course. Finally, the airway (typically the lower trachea) may be narrowed to a variable degree. This finding is best appreciated on axial CTA and axial black blood MRA images.

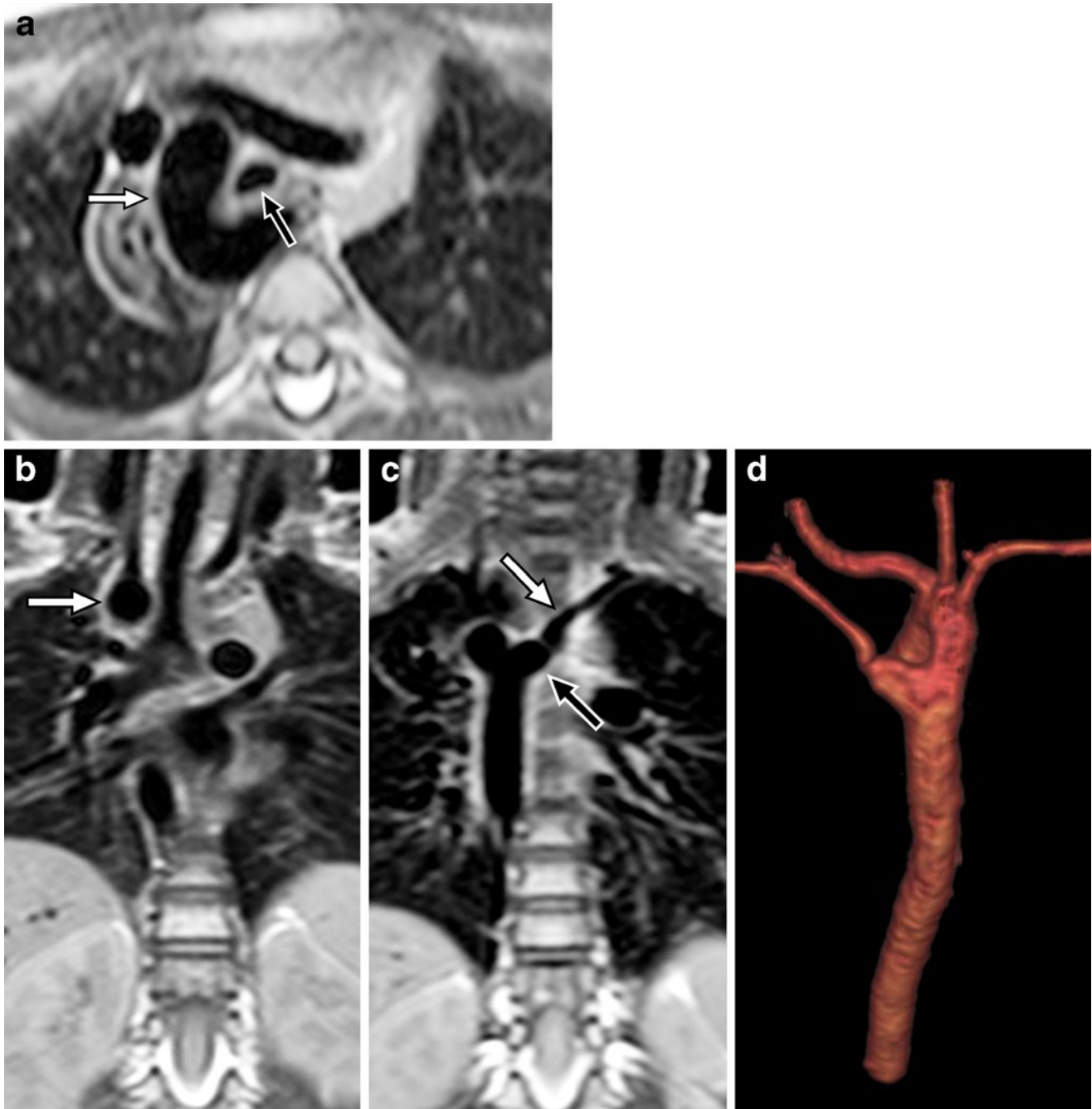


Fig. 13 Right aortic arch and aberrant left subclavian artery in a 2-year-old boy. **a** an axial black blood MR image demonstrates a right aortic arch (*white arrow*) and mild tracheal narrowing (*black arrow*). **b** A coronal black blood image confirms that the aortic arch is on the

right (*arrow*). **c** Another coronal image shows an aberrant retroesophageal left subclavian artery (*white arrow*) arising from an aortic diverticulum (*black arrow*). **d** A 3-D volume-rendered MRA image (posterior view) confirms these findings

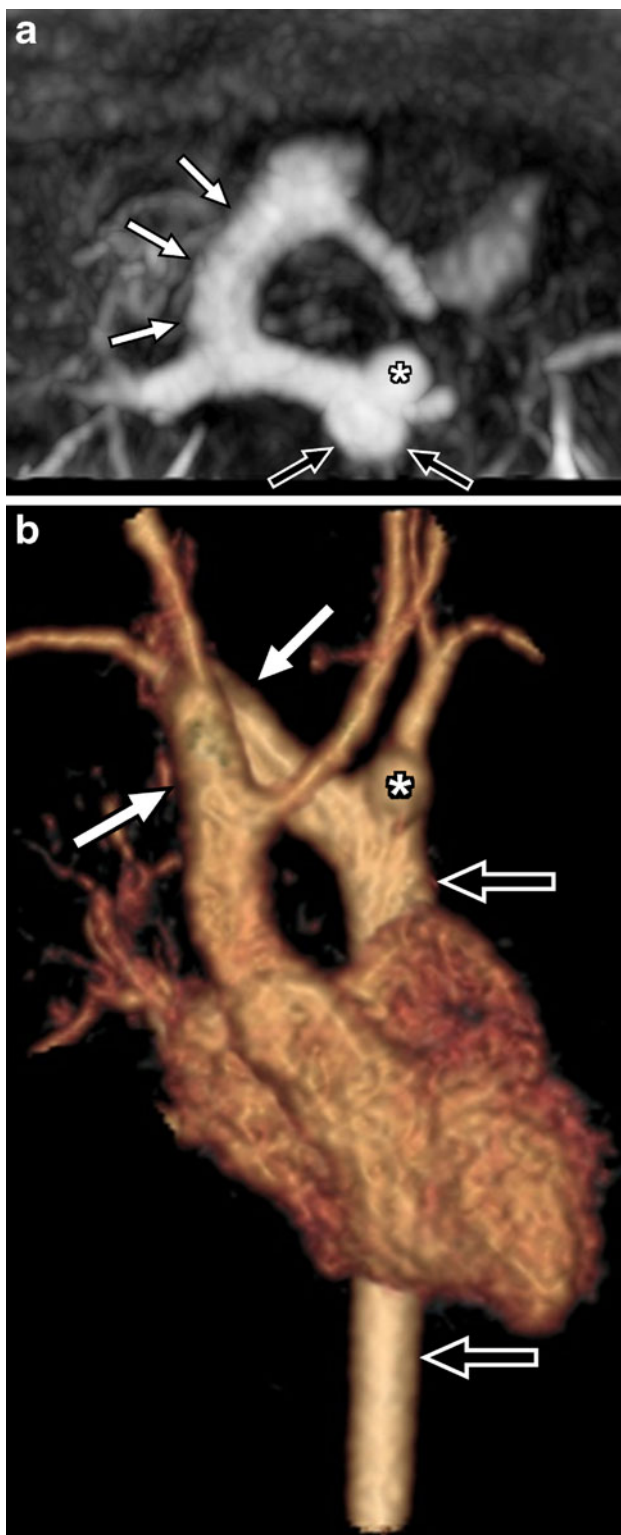


Fig. 14 Right circumflex retroesophageal aortic arch in a 21-month-old boy. **a** Axial subvolume MIP and **(b)** 3-D volume-rendered MRA images demonstrate a right aortic arch (*white arrows*) that passes retroesophageal before descending on the left (*black arrows*). The left subclavian artery arises aberrantly from a diverticulum (*) of the proximal descending thoracic aorta. An intact ligamentum arteriosum (between the left pulmonary artery and aortic diverticulum) completes the vascular ring

Uncommon vascular rings

Several additional aortic arch congenital anomalies can also result in the presence of a vascular ring. Such *uncommon* vascular rings include circumflex retroesophageal aortic arch (the ascending and descending aorta reside on different sides of the spine, while a portion of the aortic arch passes retroesophageal) (Figs. 14 and 15) [1, 2, 15–18], right cervical aortic arch with left descending thoracic aorta and aberrant left subclavian artery (with patent left ductus arteriosus or intact left ligamentum arteriosum) (Fig. 16) [19], left cervical aortic arch with right descending thoracic aorta and aberrant right subclavian artery (and patent right ductus arteriosus or intact right ligamentum arteriosum) (Fig. 17), left aortic arch with aberrant right subclavian artery and intact right ligamentum arteriosum [2, 12], right aortic arch with aberrant innominate artery [2], and right aortic arch with mirror-image branching and intact retroesophageal left ligamentum arteriosum (Fig. 18) [2, 11–13].

Both CTA and MRA can establish the presence of uncommon vascular rings as well as identify the location of

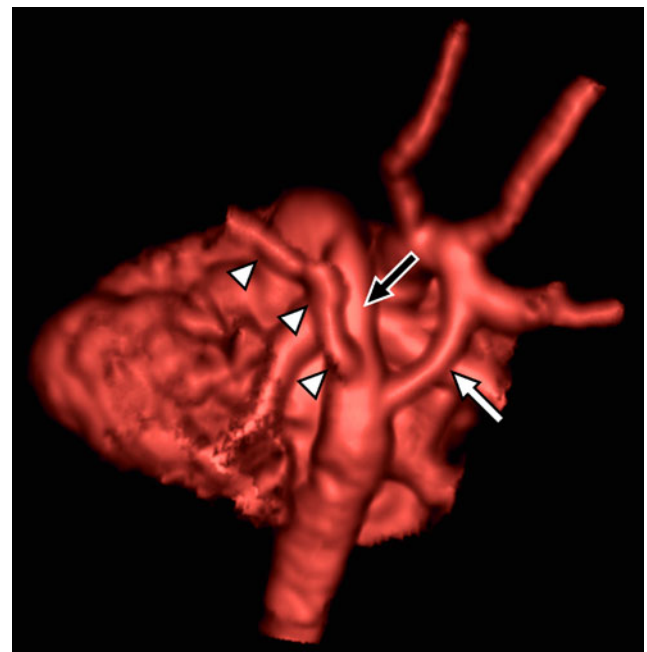


Fig. 15 Images in a 2-day-old girl with Down syndrome and a right circumflex retroesophageal aortic arch. A 3-D volume-rendered MRA image (posterior view) reveals that the retroesophageal portion of the aortic arch is hypoplastic (*white arrow*), while a large patent ductus arteriosus (*black arrow*) completes the vascular ring. The left subclavian artery (*arrowheads*) arises aberrantly from the posterior portion of the primitive right aortic arch, a structure that will eventually become an aortic diverticulum following closure of the ductus arteriosus

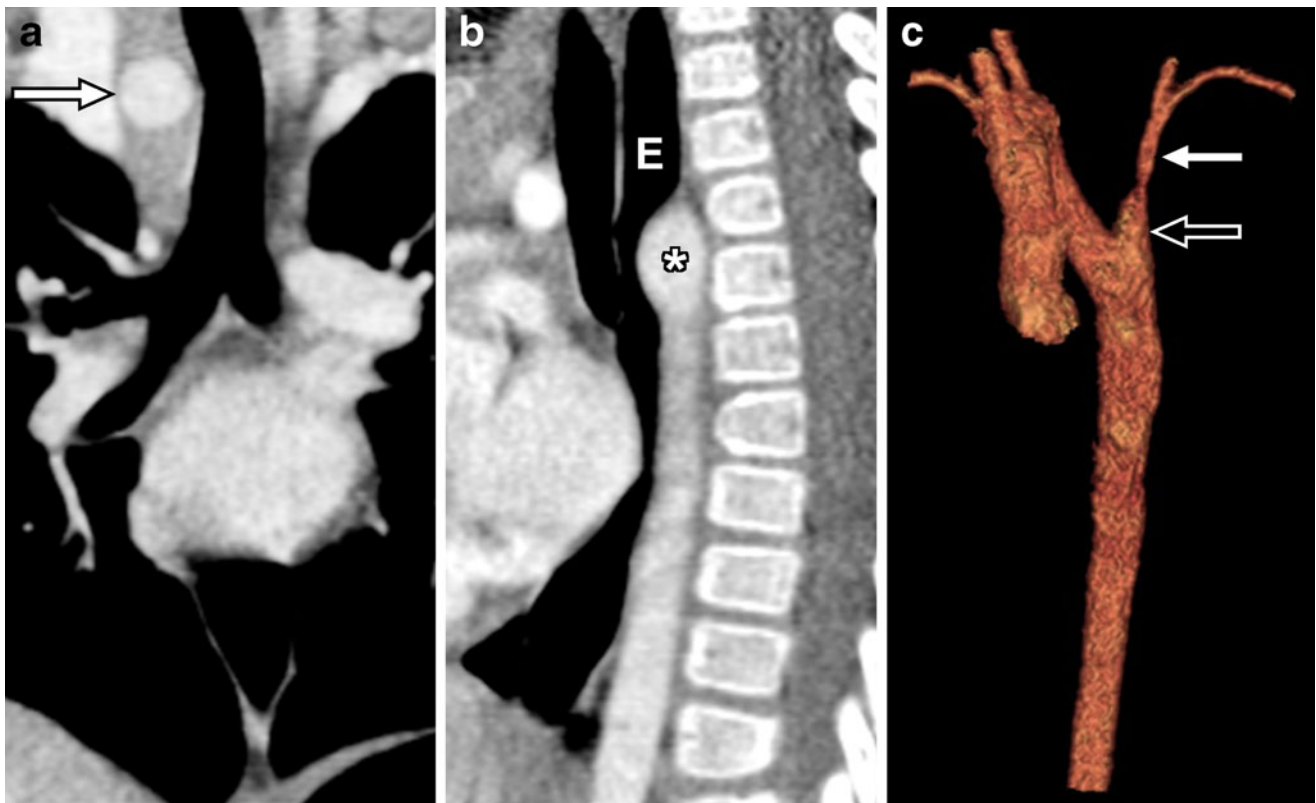


Fig. 16 Images in a 3-year-old girl with DiGeorge syndrome, a right cervical aortic arch and a vascular ring. **a** A coronal reformatted CTA image confirms that the aortic arch is located on the right at the level of the thoracic inlet (arrow). **b** A sagittal reformatted CTA image

shows the aorta (*) passing posterior to the gas-filled esophagus (E) and descending on the left. **c** A 3-D volume-rendered CTA image confirms these findings. The left subclavian artery (white arrow) arises anomalously from an aortic diverticulum (black arrow)

a contrast-filled patent ductus arteriosus or ligamentum arteriosum. While a ligamentum arteriosum typically cannot be directly visualized by imaging, its location can often be inferred based on the morphology of the vascular ring and how associated vascular structures interact with the airway. Certain aortic arch branching patterns, particularly in the setting of an aortic diverticulum, may predict the specific location (or at least sidedness) of the ligamentum arteriosum (for example, right aortic arch with mirror-image branching, associated aortic diverticulum, and an intact retroesophageal left ligamentum arteriosum) (Fig. 18). The presence of abnormal focal tracheal narrowing or asymmetry/distortion (for example, asymmetrical flattening of the trachea) also provides additional indirect corroboratory evidence of a vascular ring.

The first three of these uncommon vascular rings are associated with the descending thoracic aorta being located on the side opposite the aortic arch, circumflex aortic arch anatomy, and an intact ligamentum arteriosum (or patent ductus arteriosus) on the side opposite of the aortic arch. The retroesophageal portion of the

circumflex aortic arch is typically transverse [2], and it may be narrowed (due to coarctation) or hypoplastic leading to left ventricular outflow obstructive symptoms (Fig. 15) [15, 18, 19]. The last vascular ring mentioned above is extremely rare (the so-called type 2 right aortic arch), and it may be distinguished from a more traditional right aortic arch with mirror-image branching and no vascular ring by the presence of an aortic diverticulum and airway narrowing (Fig. 18). Most right aortic arches with mirror imaging branching do not form a vascular ring as the ligamentum arteriosum is either on the right side or passes from the left innominate artery to the left pulmonary artery.

Pulmonary sling

A pulmonary sling is diagnosed when the left pulmonary artery arises anomalously from the right pulmonary artery, passing over the right main bronchus and coursing between the trachea and esophagus to reach the left pulmonary hilum (Fig. 19) [1, 3, 5–8]. This congenital vascular anomaly is

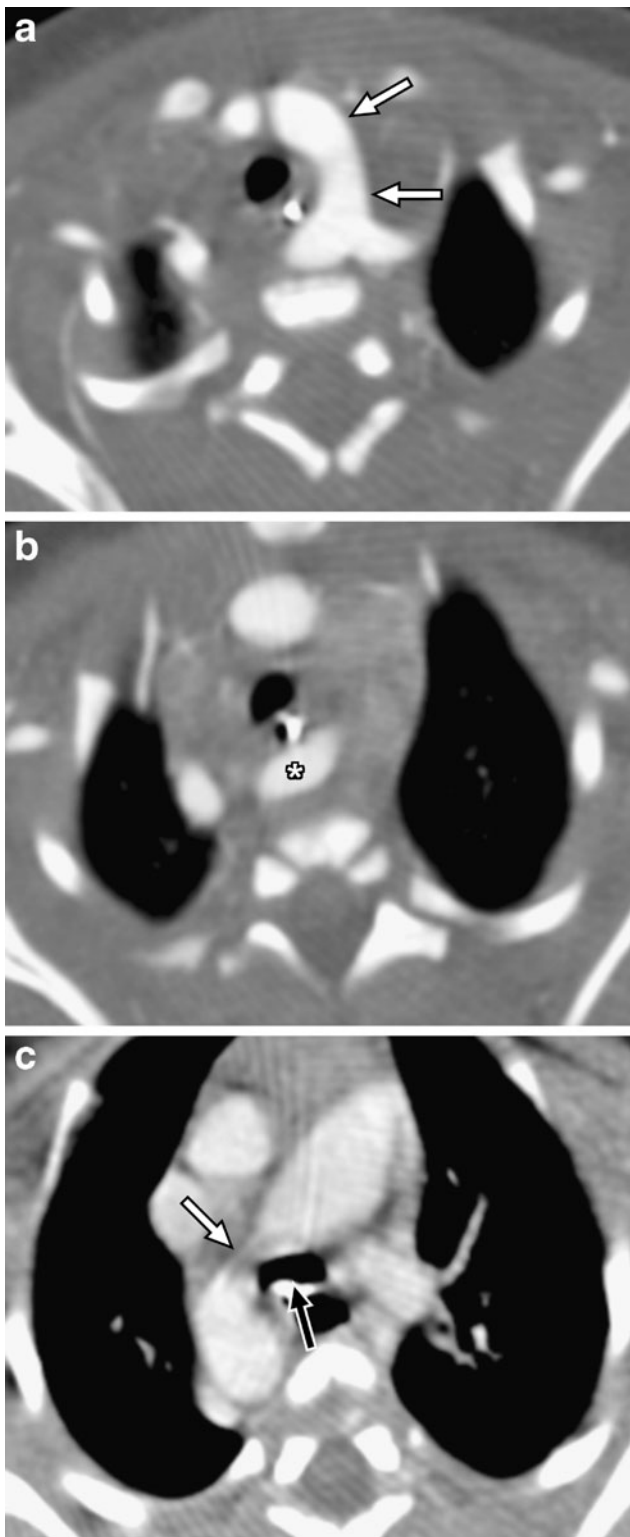


Fig. 17 Left cervical aortic arch and vascular ring in a 1-day-old girl. **a** Axial CTA image demonstrates that the aortic arch is on the left side (arrows). **b** The descending thoracic aorta (*) passes posterior to the esophagus and descends on the right. **c** A patent right ductus arteriosus (white arrow) is seen at a slightly lower level. The right subclavian artery arises anomalously from an aortic diverticulum (not shown), and the airway is mildly narrowed (black arrow)

thought to be due to abnormal obliteration or failure of development of the left 6th aortic arch [20], and it may be associated with congenital heart disease [6, 7]. Pulmonary slings most commonly present in the first year of life with respiratory symptoms [6], such as stridor, wheezing or recurrent pneumonia. These respiratory issues can be due to a variety of tracheobronchial tree abnormalities, including focal or long-segment tracheobronchial stenosis due to complete tracheal rings (the tracheal cartilage posterior membranes are absent), tracheobronchomalacia and extrinsic compression of the airway by the anomalous pulmonary artery [6]. The presence of complete tracheal rings may be suggested by an unusually round appearance of the airway, airway narrowing, and lack of change in airway caliber between inspiration and expiration [8].

There have been attempts to classify pulmonary slings based on the associated airway abnormalities [5–7, 21]. In *type I* pulmonary slings, there is often a normal airway branching pattern with compression of the trachea and right mainstem bronchus by the anomalous left pulmonary artery. This form of pulmonary sling is associated with overall lower morbidity and decreased mortality, and may (*type IB*) or may not (*type IA*) be associated with a tracheal (porcine) bronchus, tracheobronchomalacia (particularly the right mainstem bronchus) and unilateral pulmonary hyperinflation [21].

With *type II* pulmonary slings, there is typically long-segment tracheobronchial stenosis, and the anomalous left pulmonary artery is more caudad in location [21]. This form is associated with overall higher morbidity and mortality during infancy, primarily related to airway narrowing [5–7, 21], and it is associated with tracheobronchial branching anomalies, including left intermediate and right bridging bronchi, a low (around the T6 thoracic spine level) “inverted T” carina, complete tracheal rings and bilateral pulmonary hyperinflation [6, 7, 9, 21].

At radiography, pulmonary slings may present with a variety of airway-related findings, including focal or long-segment tracheal narrowing, “inverted T” appearance of the carina, and anterior deviation of lower trachea and carina on lateral imaging (Fig. 20) [3, 6, 9, 21]. Unilateral or bilateral pulmonary overinflation may be observed due to airway narrowing and air-trapping (Fig. 20) [1, 6, 9]. An abnormal smooth rounded anterior esophageal indentation is present without abnormal lateral or posterior indentations at esophagography (Fig. 21) [1, 3, 6, 9].

Both CTA and MRA can depict pulmonary slings and associated airway abnormalities (Figs. 22 and 23) [6, 7, 20]. First, the anomalous left pulmonary artery can be seen arising from the right pulmonary artery, passing between

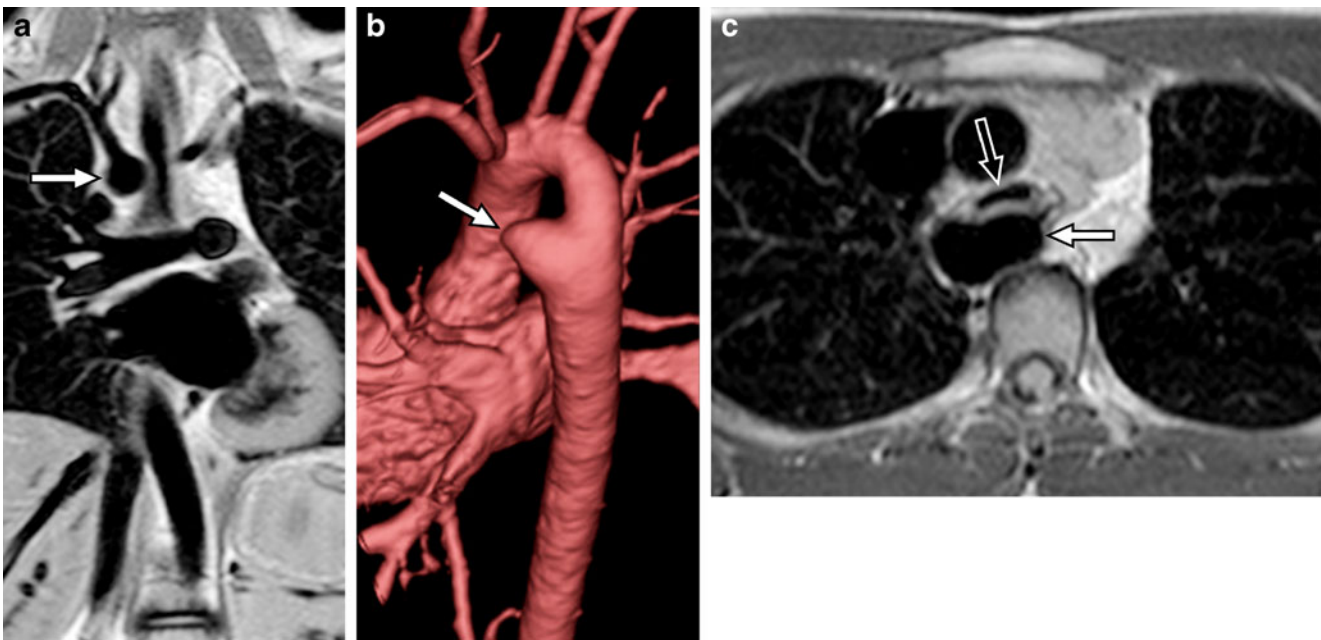


Fig. 18 Right aortic arch and vascular ring in a 13-year-old girl. **a** Coronal black blood MRI image reveals a right aortic arch (*arrow*). **b** A 3-D volume-rendered MRA image (posterior view) demonstrates a right aortic arch with mirror image branching as well as an aortic

diverticulum (*arrow*). **c** An axial black blood image confirms the presence of a large aortic diverticulum (*white arrow*) suggesting the presence of an intact retroesophageal left ligamentum arteriosum. The trachea is severely narrowed (*black arrow*)

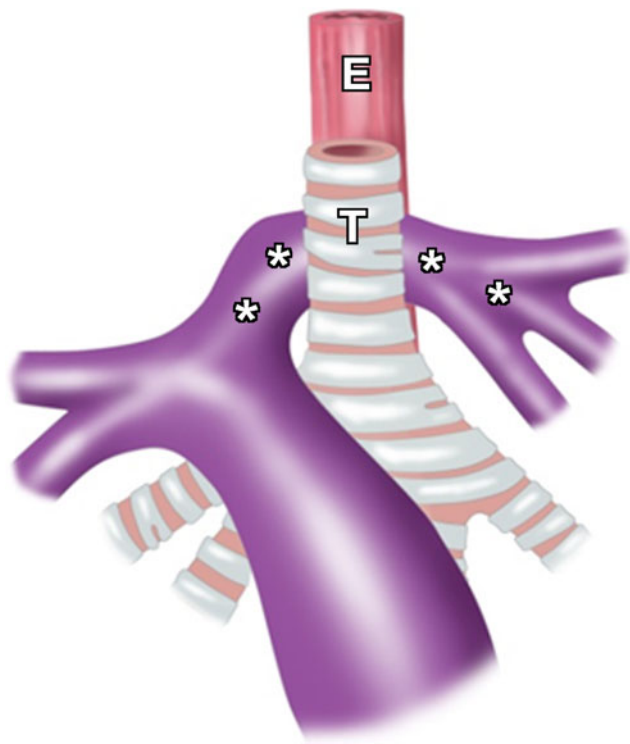


Fig. 19 Illustration of pulmonary sling. The left pulmonary artery (*) arises anomalously from the central right pulmonary artery and passes between the trachea (T) and esophagus (E)

the esophagus and trachea. Both CTA and MRA can also assess the caliber of the anomalous left pulmonary artery and evaluate for abnormal pulmonary artery narrowing. Second, both imaging modalities can be used to evaluate the central airway to assess for tracheobronchial anomalies and abnormal narrowing. This information is particularly important for planning often very complex surgical tracheal reconstruction procedures. The airways are best visualized on coronal reformatted and volume-rendered CTA images as well as axial and coronal thin-section, high-resolution black blood and 3-D SSFP MRA images. Finally, both CTA and MRA allow for the assessment of overall lung size to evaluate for evidence of air-trapping.

Pulmonary sling variants

Rarely, a pulmonary sling is associated with diffuse hypoplasia of the pulmonary arterial tree (Fig. 24). Pulmonary sling anatomy with passage of the left pulmonary artery between the trachea and esophagus may also be observed in the setting of right unilateral pulmonary agenesis (Fig. 25) [8, 20]. In this latter condition, the left pulmonary artery arises from the main pulmonary artery as the right pulmonary artery is congenitally absent [8].

Fig. 20 Airway findings in a child with a pulmonary sling. **a** Chest radiograph in a 6-month-old girl with a pulmonary sling and left lung air trapping due to airway narrowing. **b** Lateral radiograph in a 1-year-old boy with a pulmonary sling and lower tracheal narrowing and anterior bowing (*arrow*) due to anomalous left pulmonary artery

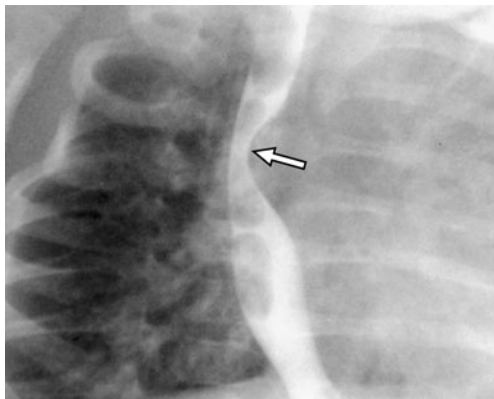
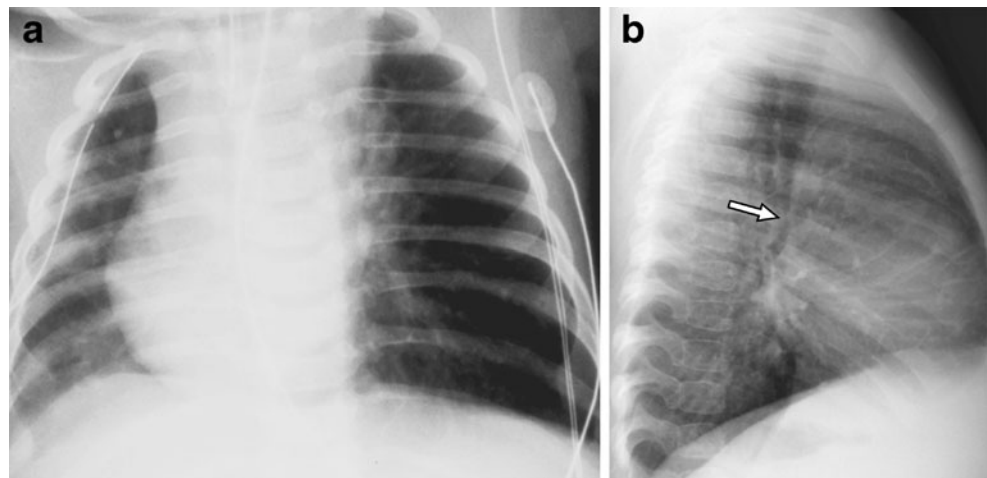


Fig. 21 Esophagography in a 10-month-old boy with a pulmonary sling and abnormal anterior esophageal indentation at esophagography (*arrow*) indentation (oblique image)

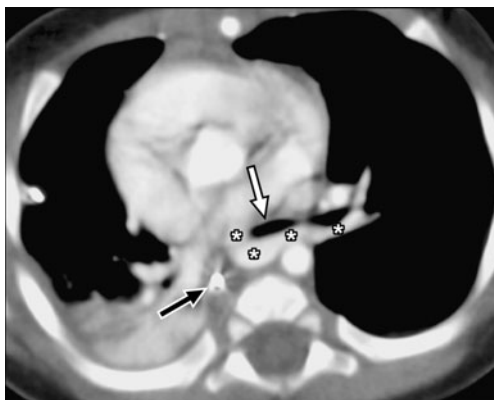


Fig. 22 Pulmonary sling in a 6-month-old girl. The left pulmonary artery (*) arises anomalously from the right pulmonary artery, and the airway is narrowed (*white arrow*) due to extrinsic compression. A nasogastric tube is within the esophagus (*black arrow*)

Summary

Vascular rings and pulmonary slings represent a heterogeneous group of congenital thoracic vascular anomalies. When symptomatic, these conditions most commonly present with respiratory and feeding difficulties early in life. As we have shown, the diagnosis of vascular rings and pulmonary slings frequently relies upon a multi-modality radiological approach. State-of-the-art CTA and MRA imaging techniques accurately depict these vascular anomalies in children of all ages and almost always eliminate the need for diagnostic catheter-based angiography.



Fig. 23 Pulmonary sling in a 2-month-old boy. An axial black blood MRI image demonstrates an anomalous origin of the left pulmonary artery (*) and marked tracheal narrowing (*arrow*)

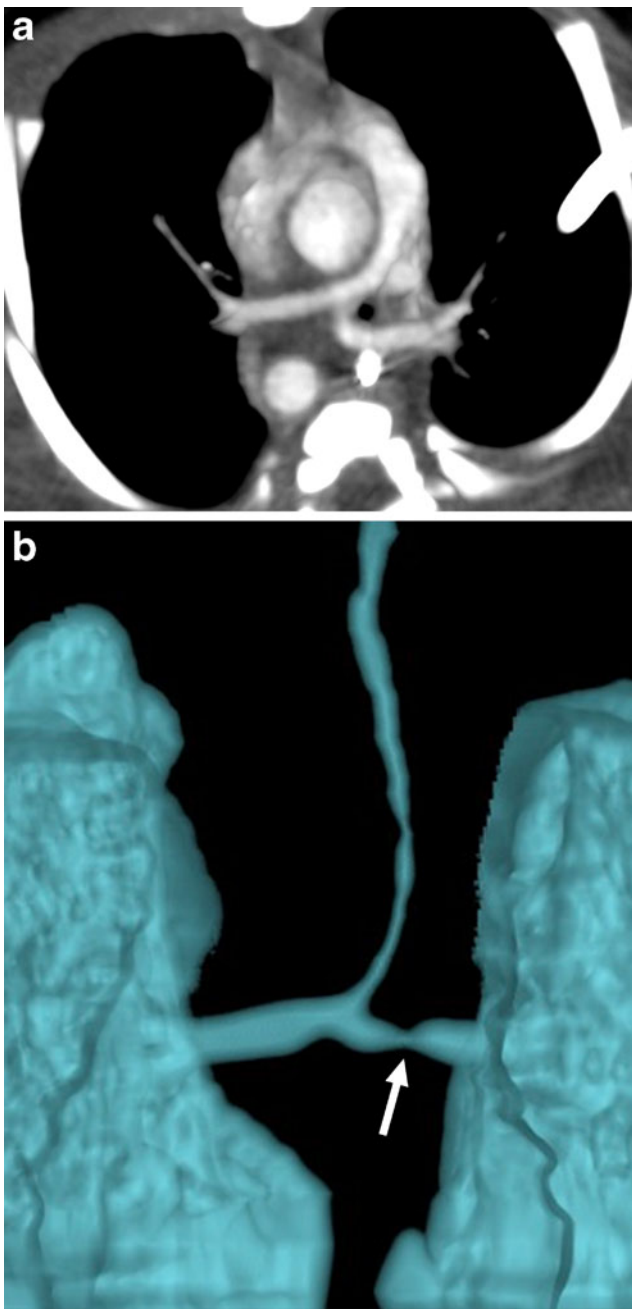


Fig. 24 Right aortic arch and type II pulmonary sling in a 1-day-old boy. **a** An axial subvolume MIP CTA image reveals diffuse pulmonary arterial hypoplasia and pulmonary sling anatomy. The trachea appears O-shaped and is narrowed. **b** A 3-D volume-rendered image of the airway demonstrates a low “inverted T” configuration of the carina, and there is severe long-segment tracheal narrowing as well as focal stenosis of the left main bronchus due to complete cartilaginous rings (*arrow*)

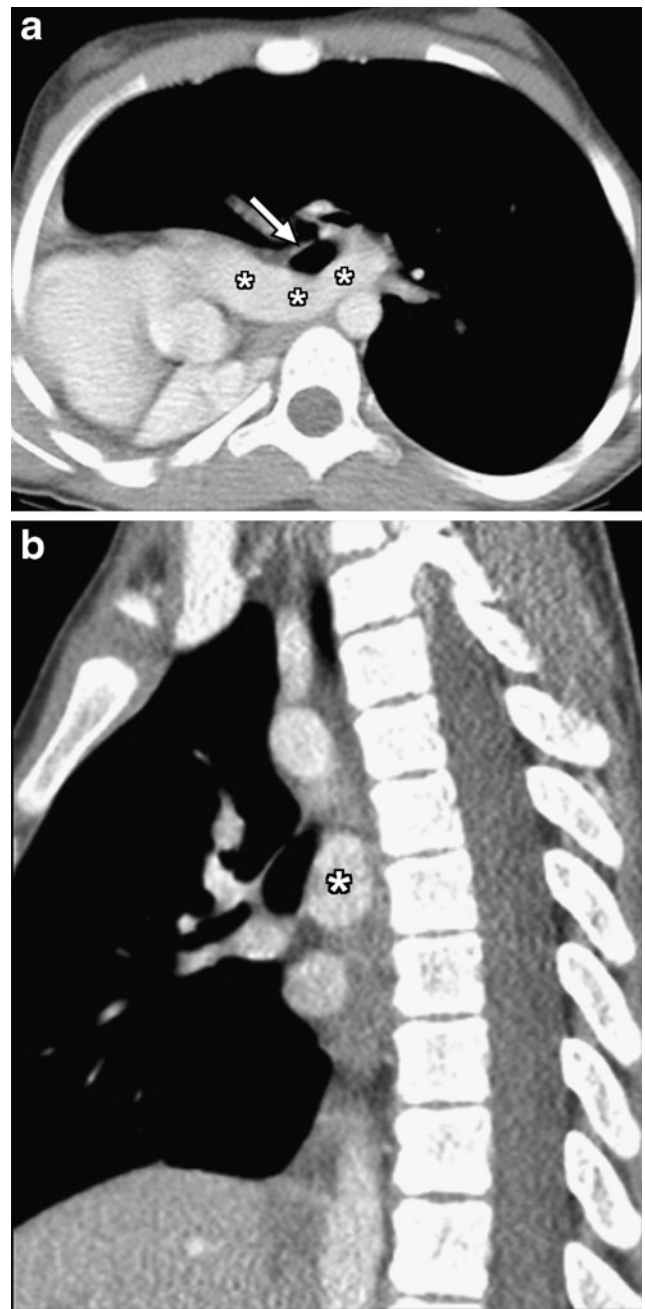


Fig. 25 Images in a 9-year-old girl with right pulmonary agenesis and pulmonary sling anatomy. **a** An axial CTA image demonstrates absence of the right lung and pulmonary artery. The left pulmonary artery (*) passes between the trachea and esophagus, and trachea is mildly narrowed (*arrow*). **b** Sagittal reformatted CTA image confirms passage of the left pulmonary artery (*) posterior to the trachea

References

1. Berdon WE, Baker DH (1972) Vascular anomalies and the infant lung: rings, slings, and other things. *Semin Roentgenol* 7:39–64
2. Hernanz-Schulman M (2005) Vascular rings: a practical approach to imaging diagnosis. *Pediatr Radiol* 35:961–979
3. Simoneaux SF, Bank ER, Webber JB et al (1995) MR imaging of the pediatric airway. *Radiographics* 15:287–298
4. Lowe GM, Donaldson JS, Backer CL (1991) Vascular rings: 10-year review of imaging. *Radiographics* 11:637–646
5. Castañer E, Gallardo X, Rimola J et al (2006) Congenital and acquired pulmonary artery anomalies in the adult: radiologic overview. *Radiographics* 26:349–371
6. Lee KH, Yoon CS, Choe KO et al (2001) Use of imaging for assessing anatomical relationships of tracheobronchial anomalies associated with left pulmonary artery sling. *Pediatr Radiol* 31:269–278
7. Zhong YM, Jaffe RB, Zhu M et al (2010) CT assessment of tracheobronchial anomaly in left pulmonary artery sling. *Pediatr Radiol* 40:1755–1762
8. Espinosa L, Agarwal P (2008) Adult presentation of right lung agenesis and left pulmonary artery sling. *Acta Radiol* 49:41–44
9. Browne LP (2009) What is the optimal imaging for vascular rings and slings? *Pediatr Radiol* 39(Suppl 2):S191–S195
10. Dillman JR, Hernandez RJ (2009) Role of CT in the evaluation of congenital cardiovascular disease in children. *AJR* 192:1219–1231
11. Kellenberger CJ (2010) Aortic arch malformations. *Pediatr Radiol* 40:876–884
12. Schlesinger AE, Mendeloff E, Sharkey AM et al (1995) MR of right aortic arch with mirror-image branching and a left ligamentum arteriosum: an unusual cause of a vascular ring. *Pediatr Radiol* 25:455–457
13. Schlesinger AE, Krishnamurthy R, Sena LM et al (2005) Incomplete double aortic arch with atresia of the distal left arch: distinctive imaging appearance. *AJR* 184:1634–1639
14. Holmes KW, Bluemke DA, Vricella LA et al (2006) Magnetic resonance imaging of a distorted left subclavian artery course: an important clue to an unusual type of double aortic arch. *Pediatr Cardiol* 27:316–320
15. Hilmes M, Hernandez R, Devaney E (2007) Markedly hypoplastic circumflex retroesophageal right aortic arch: MR imaging and surgical implications. *Pediatr Radiol* 37:63–67
16. Dominguez R, Oh KS, Dorst JP et al (1978) Left aortic arch with right descending aorta. *AJR* 130:917–920
17. McLeary MS, Frye LL, Young LW (1998) Magnetic resonance imaging of a left circumflex aortic arch and aberrant right subclavian artery: the other vascular ring. *Pediatr Radiol* 28:263–265
18. Ahluwalia GS, Rashid AG, Griselli M et al (2007) Hypoplastic circumflex retroesophageal right-sided cervical aortic arch with unusual vascular arrangement and severe coarctation. *Ann Thorac Surg* 84:1014–1016
19. Ahn KS, Yong HS, Lee JW et al (2007) Right circumflex retroesophageal aortic arch with coarctation of a high-positioned right arch. *Pediatr Radiol* 37:584–586
20. Pu WT, Chung T, Hoffer FA et al (1996) Diagnosis and management of agenesis of the right lung and left pulmonary artery sling. *Am J Cardiol* 78:723–727
21. Wells TR, Gwinn JL, Landing BH et al (1988) Reconsideration of the anatomy of sling left pulmonary artery: the association of one form with bridging bronchus and imperforate anus. Anatomic and diagnostic aspects. *J Pediatr Surg* 23:892–898

Copyright of Pediatric Radiology is the property of Springer Science & Business Media B.V. and its content may not be copied or emailed to multiple sites or posted to a listserv without the copyright holder's express written permission. However, users may print, download, or email articles for individual use.